

Adaptive hysteresis band current control of grid connected PV inverter

R. S. Ravi Sankar, A. Venkatesh, Deepika Kollipara

Department of Electrical and Electronics Engineering, Vignan's Institute of Information Technology,
Andhra Pradesh, India

Article Info

Article history:

Received Jul 18, 2020

Revised Nov 23, 2020

Accepted Dec 19, 2020

Keywords:

Adaptive hysteresis band
controller

DC link

Perturb and observe method

Voltage source converter

Voltage source inverter

ABSTRACT

In this paper, adaptive hysteresis band current controller is implemented to control the current injected into the grid. Initially it was implemented by B.K Bose for control of the machine drive. Now it is implemented for the grid connected PV inverter, to control the current injected into Grid. It is well suitable for the distribution generation. The adaptive hysteresis band controller changes the bandwidth based on the modulating frequency, supply voltage, input DC voltage and slope of the reference current. Consequently, the controller generates pulses to the inverter. It is advantageous over the conventional hysteresis controller, as the switching frequency is maintained almost constant. Thereby quality of grid current is also improved. It is verified in time domain analysis of simulation using MATLAB.

This is an open access article under the [CC BY-SA](https://creativecommons.org/licenses/by-sa/4.0/) license.



Corresponding Author:

R. S. Ravi Sankar

Department of Electrical and Electronics Engineering

Vignan's Institute of Information Technology

Vishakapatnam, Andhara Pradash, 530046, India

Email: satya_ravi2001@yahoo.com

1. INTRODUCTION

Due to the development of power electronic device in power system generates the harmonics in voltage as well as current power high frequency which effect the performance of the loads. These are crucial role in power quality issues. There was a technical improvements are there in HVDC and FCTS device to reduce the generation of harmonics [1]. The VSC based converter are used in medium and low level power transmission for high level power SCR based HVDC system is used [2-5]. HVDC DC light is made of fully controlled switch such as IGBT or MOSFET along with PWM technique. It reduces the harmonic generation, minimizes the filter requirements [6, 7]. The HVDC system is a highly efficient alternative for transmitting large amounts of electricity over long distances and for special purpose applications. As a key enabler in the future energy system based on renewables, HVDC is truly shaping the grid of the future [8]. This hierarchical control structure is discussed which is important tool to maintain the dynamics, stationery performance of the micro grid with respective economical aspects [9]. Different control schemes are discussed in DC micro-Grid to mitigate the issues in it with the goal of providing control design guild lines [10, 11]. The high bandwidth hierarchical control structure for AC micro grid in distribution level. Conventionally to control Grid voltage and frequency were done by hierarchical linear control loops. they suffer from slow response with parametric effects. So the model predictive control technique is used to realize with heigh band width to control the multiple VSC. Furthermore, droop control and virtual impedance methods were employed to share active and reactive power. Based on a large-signal dynamic model of a micro grid, a linear parameter varying based state estimator that is localized in each distributed generation (DG) unit serves as an alternative

communication role and obtains the dynamics of the other DG units independently. A linear matrix inequality formulation for pole placement condition was derived for the state estimator design. A decentralized secondary voltage controller is, thus, able to achieve accurate reactive power sharing and average voltage restoration without any additional communication links [12]. A novel system operation strategy with energy management system was proposed in DC micro grid with different energy storage system where high penetration of renewable energy source. In both islanded and grid connected operation strategy of the micro grid, the ultra-capacitor unit has vital role to support the dc link. The micro-grid was controlled to deliver/absorb certain amount of power to grid. No power is dispatched to the grid in island mode [13].

In hysteresis controller, the error band is normally fixed to a certain value. Consequently, the switching frequency varies within a band because peak to peak of ripple current must be controlled at all points of the fundamental frequency wave. Adaptive hysteresis band current controller changes the hysteresis bandwidth according to the reference current to make switching frequency of inverter nearly constant and further reduces the THD of supply current. Adaptive hysteresis band current controller was used as current control method [14]. In section 2 modeling of the PV system with MPPT technique, hysteresis and adaptive hysteresis current control of the grid tied inverters with detailed modelling is presented. In Section 3 simulation results of hysteresis and adaptive hysteresis band controllers are inspected and compared in terms of % THD in grid current.

2. DESIGN AND IMPLEMENTATION OF THE SYSTEM

2.1. Design of the PV array

PV array is the combination of the PV modules. The primary element is PV cell, which converts the solar power to electrical power. Different modelling of the PV cell is given in literature survey such as single diode model, two diode models, and multiple diode models. In this paper two diode model of the PV cell is considered is shown in Figure 1. I_{pv} is the photo current. D1 and D2 are two anti-parallel diodes, R_p is leakage resistance and R_s is contact resistance. V is the output voltage of single cell and the output current of cell 'I' is given in (1) [15-19].

$$I = I_{pv} - I_{D1} - I_{D2} - \left(\frac{V + IR_s}{R_p} \right) \quad (1)$$

$$I_{D1} = I_{o1} \left[\exp\left(\frac{q(V + IR_s)}{A_1 KT} \right) - 1 \right] \quad (2)$$

$$I_{D2} = I_{o2} \left[\exp\left(\frac{q(V + IR_s)}{A_2 KT} \right) - 1 \right] \quad (3)$$

$$I_{pv} = [I_{scr} + K_i(T_k - T_{refk})] \times \lambda / 1000 \quad (4)$$

Here λ is solar irradiation, I_{scr} is short current of PV cell, T_k and T_{refk} are the actual and standard temperatures respectively. K is temperature coefficient of short-circuit current (A/ K), A_1 and A_2 are the ideality factors of the diodes. q is the charge of the electron, I_{o1} and I_{o2} are the reverse saturation currents of diodes D1, D2 respectively. As shown in (1) is modified for PV module as given in (5).

$$I = N_p I_{pv} - N_p I_{D1} - N_p I_{D2} - \left(\frac{V + IR_s}{R_p} \right) \quad (5)$$

In equation substitute the (1) and (3).

$$I = N_p \times I_{pv} - N_p \times I_{o1} \left[\exp\left\{ \frac{q \times (V + IR_s)}{N_s A_1 k T} \right\} - 1 \right] - N_p \times I_{o2} \left[\exp\left\{ \frac{q \times (V + IR_s)}{N_s A_2 k T} \right\} - 1 \right] - \left(\frac{V + IR_s}{R_p} \right) \quad (6)$$

Here N_s and N_p are the No. of cells are cascaded and shunted in module. These modules are connected in cascade and shunt to meet the voltage and power rating. PV array current is given in (7).

$$I = N_{pp} \times I_{pv} - N_{pp} \times I_{o1} \left[\exp\left\{ \frac{q \times (V + IR_s \left(\frac{N_{ss}}{N_{pp}} \right))}{N_s A_1 k T} \right\} - 1 \right] - N_{pp} \times I_{o2} \left[\exp\left\{ \frac{q \times (V + IR_s \left(\frac{N_{ss}}{N_{pp}} \right))}{N_s A_2 k T} \right\} - 1 \right] - \left(\frac{V + IR_s \left(\frac{N_{ss}}{N_{pp}} \right)}{R_p \left(\frac{N_{ss}}{N_{pp}} \right)} \right) \quad (7)$$

Where N_{ss} and N_{pp} are the number of series connected modules and parallel connected series strings in PV array respectively. The standard KC200GT data sheet parameters are used for PV array simulation are given

in Table 1. To extract the maximum power from PV array due to changes in atmospheric conditions. The different control techniques are presented in literature such as Incremental conductance method, perturb and observe method, and current sweep and constant voltage. Perturb and Observe method finds the change in output power of the PV panel. If the change power is positive, panel voltage will increase, otherwise panel voltage decreases. It is achieved with the help of the boost converter [20-22]. Generally, a DC-DC boost converter is used to extract the maximum power from the PV array. It is shown Figure 2. The inductor stores the energy when switch is ON, the stored energy is released to the load when it is OFF.

The design the parameters of the boost converter is given in (8).

$$DutyCycleD = 1 - \frac{V_o}{V_s}; Induc\ tan\ c\ eL = \frac{V_s D}{\Delta I f} \text{ Capaci\ tan\ c\ eC} = \frac{I_{o\ r\ e\ f\ e\ r\ e\ n\ c\ e} D}{\Delta V f} \tag{8}$$

Where, V_s =Source voltage, V_o =Output voltage, D =Duty cycle, ΔI =Ripples in current, ΔV =Ripples in output voltage.

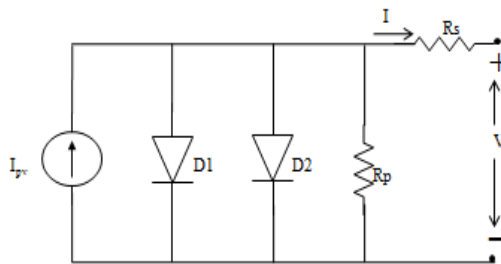


Figure 1. Equivalent circuit of a PV cell

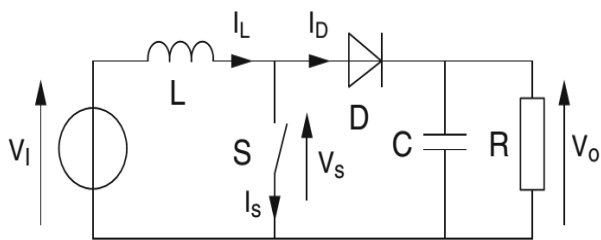


Figure 2. Boost converter circuit

Table 1. Parameters of the PV module

Parameter	Variable	Value
Current at maximum power	Im	8.30 A
Voltage at maximum power	Vm	30.2 V
Open circuit voltage	Voc	37.3 V
Short circuit current	Isc	8.71 A
Series resistance	Rs	0.217 ohm
Reference solar radiation	Sref	1000 W/m ²
Reference temperature	Tref	300 k

2.2. Perturb and observe method

In this work the DC link is derived from the PV array, due to uncertainties in the climatic conditions. The power from PV panel is variable. To extract the maximum power from the PV panel, different MPPT methods are proposed in literature. Such as fixed duty cycle method, beta method, Incremental conductance method, perturb and observe method, constant voltage current method, and fractional voltage method. Each method has its own advantages and disadvantages. In this paper perturb and observe (P&O) method is used due to the easy implementation [23].

2.3. Operation of 3-phase inverter

Currently 3-phase inverters are predominantly used in both AC/DC Microgrid operations. A 3-phase inverter consist of six switches as shown in the Figure 3. When upper device is ‘ON’, the load terminals are connected to the positive voltage and when lower device is ‘ON’, the load is connected to the negative terminal voltage. Applying proper pulses to the switches three phase voltage is generated, that is applied to the grid through a filter. To filter out the harmonics in the current, different filters ‘L’, ‘LCL’, ‘LC’ are available in literature [24]. ‘L’ filter was used to filter the harmonics in the current [25-26].

2.4. Hysteresis band controller

In this current control technique, actual grid current is compared to reference current as shown in Figure 4. If error current is more than the fixed band then the switches are turned ‘on’. If it is less than the lower limit, then lower switches in the respective phases are turned ‘on’. Thereby the grid current is restricted within the set limits. The harmonics presented in the grid current depends highly on the selected band for

controller, type of the filter and its value. One of the main disadvantages of this controller is variable switching frequency due the fixed bandwidth. It is difficult to design the filter at variable frequency. This is overcome with a novel hysteresis current controller. Its design and implementation is discussed in the next section of this paper. The circuit diagram of the system with this controller is shown in Figure 3 [27].

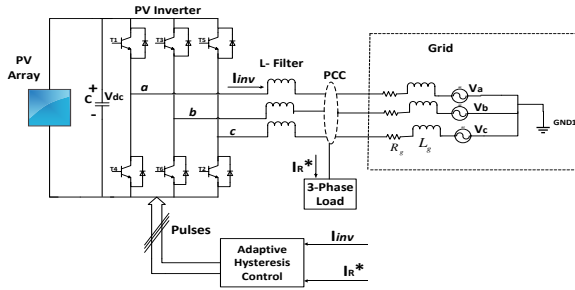


Figure 3. 3-Ph inverter connected to the grid

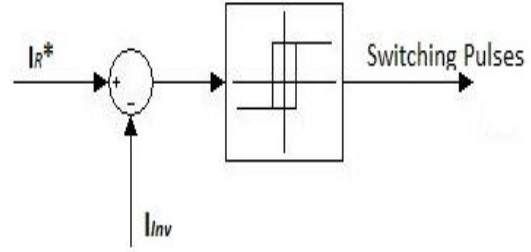


Figure 4. Hysteresis controller

2.5. Adaptive hysteresis band current controller

The switching pattern of the single phase of the 3-ph. inverter is described below. Conventional hysteresis current controller.

$$I_{INV} \geq (I_R - HB) \text{ Then T1 is ON \& T4 is OFF} \tag{9}$$

$$I_{INV} \geq (I_R + HB) \text{ Then T1 is OFF \& T4 is ON}$$

The switching frequency of the hysteresis fixed band controller depends on the how fast inverter current changes from the upper limit to the lower limit and vice-versa. Slope of the inverter current depends on the filter value and DC input voltage of the grid connected inverter. Accordingly, the switching frequency varies [28].

Bandwidth of the hysteresis controller allows the inverter current error. By varying the bandwidth, variation in switching frequency can be achieved. As the switching frequency increases, the switching loss of the inverter and subsequently, electromagnetic interference (EMI) increases. So while selecting the bandwidth for a hysteresis controller, the above mentioned parameters are compromised. Hysteresis controller is simple to implement among PWM converters. It has inherent peak current limiting control and it does not require any system information. However, it suffers from variable frequency. Improved version of this technique is implemented for shunt active filters and drives [29-31]. In case of the adaptive hysteresis band controller, the band width of the hysteresis controller will be updated depending on the DC voltage, slope of the reference current, and filter values and grid voltage. as detailed in (10)-(19).

$$\frac{dI_{INV}^+}{dt} = \frac{1}{L} (V_{DC} - V_S) \tag{10}$$

$$\frac{dI_{INV}^-}{dt} = -\frac{1}{L} (V_{DC} + V_S) \tag{11}$$

From the geometry of the Figure 5,

$$\frac{dI_{INV}^+}{dt} t_1 - \frac{dI_R^+}{dt} t_1 = 2HB \tag{12}$$

$$\frac{dI_{INV}^-}{dt} t_2 - \frac{dI_R^-}{dt} t_2 = -2HB \tag{13}$$

$$t_1 + t_2 = T_c = \frac{1}{f_c} \tag{14}$$

Add (12) and (13) and substitute in (14).

$$\frac{dI_{INV}^-}{dt} + \frac{dI_{INV}^+}{dt} - \frac{1}{f_c} \frac{dI_R^*}{dt} = 0 \tag{15}$$

Subtract (12) and (13), we get;

$$\frac{dI_{INV}^-}{dt} - \frac{dI_{INV}^+}{dt} - (t_1 - t_2) \frac{dI_R^*}{dt} = 4HB \tag{16}$$

Substitute (14) in (16). It results into;

$$(t_1 + t_2) \frac{dI_{INV}^-}{dt} - (t_1 - t_2) \frac{dI_R^*}{dt} = 4HB \tag{17}$$

Substitute the (14) in (17) and simplify;

$$t_2 - t_1 = \frac{dI_R^*/dt}{f_c(I_{INV}^+/dt)} \tag{18}$$

From above equations, the hysteresis band is given (19).

$$HB = \left\{ \frac{0.125V_{DC}}{f_c L} \left[1 - \frac{4L^2}{V_{DC}^2} \left(\frac{V_S}{L} + m \right) \right] \right\} \tag{19}$$

where;

f_c : Switching frequency

m : Slope of the inverter current.

Adaptive hysteresis band current controller changes the bandwidth depending on the slope of the inverter current and DC voltage. It reduces the influence of current distortion on the reference wave. The expression for the HB is given in the equation. The simple block diagram of the adaptive hysteresis band current controller is given in Figure 6.

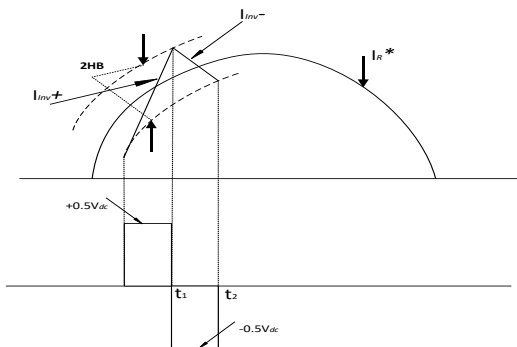


Figure 5. Geometry of the reference and actual current

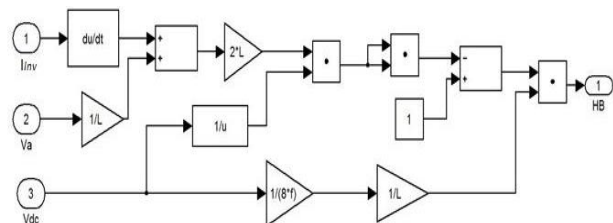


Figure 6. Simulation of the adaptive HB

3. SIMULATION RESULTS

Simulation waveform of PV array voltage is shown in Figure 7, where the output voltage is 380 V upto 0.5 Sec. Due to change in temperature at 0.5 sec, voltage raises to around 480 V. The current and power supplied by the PV module is shown in Figure 8 and Figure 9 respectively. It is observed in Figure 9, that the current as well power supplied by the PV also changes at 0.5 sec. It is due to the constant reference current to the PV inverter.

Output voltage and current of the inverter are illustrated in Figure 10. It can be noticed that 3-ph. inverter output is changed at 0.5 sec. This is due to change in DC link voltage. Reference current is taken as 4 A. THD of the grid current with adaptive hysteresis controller is shown in Figure 11. THD of the grid current with Hysteresis controller is depicted in Figure 12. It is observed that THD is improved to 2.34% with adaptive hysteresis controller in comparison with 3.19 with hysteresis controller.

THD of the inverter current for the different reference currents values are tabulated in the Table 2. without changing the system parameters, the adaptive hysteresis band controller has given the less THD of the current, compare to the hysteresis controller. The voltage across switch is shown Figure 13. with hysteresis current controller. The time period of the switch is not constant and more ever the switch frequency is low. The adaptive hysteresis band controller the switching time low, means the switching frequency is high, where which requires the low value of the filter, is also constant shown Figure 14.

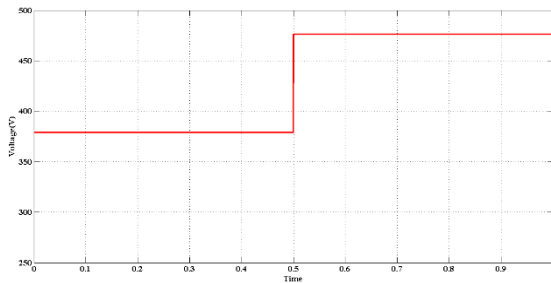


Figure 7. PV voltage

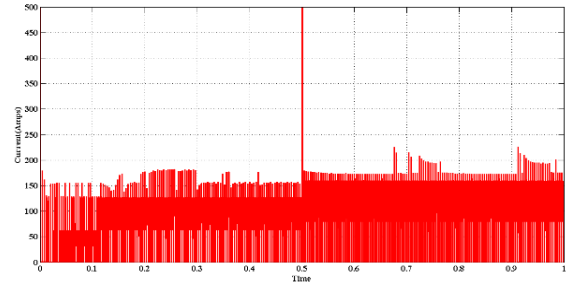


Figure 8. PV current

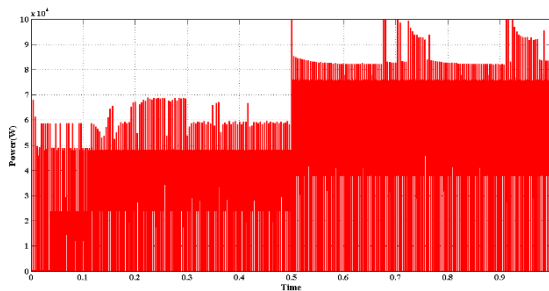


Figure 9. PV power

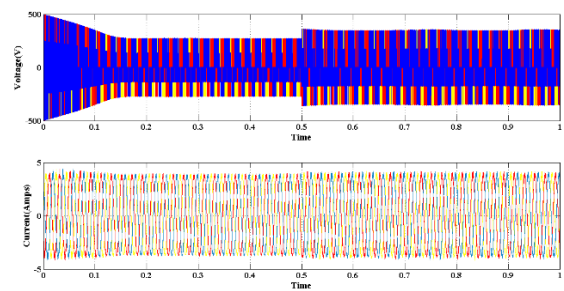


Figure 10. Inverter voltage and inverter current

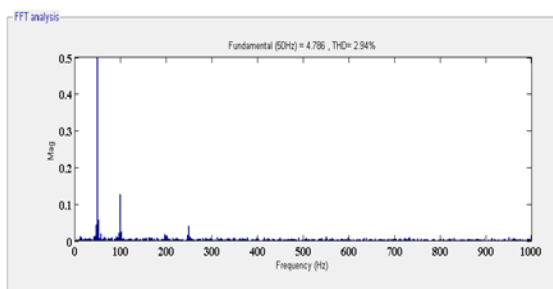


Figure 11. THD of the grid current with adaptive hysteresis controller (5A)

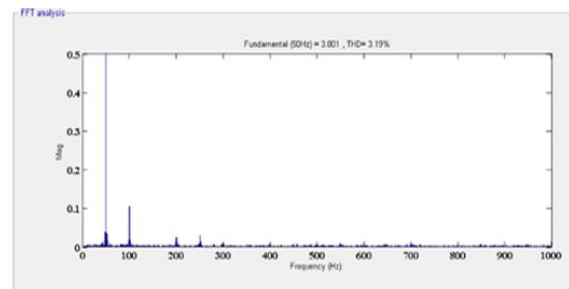


Figure 12. THD of grid current with hysteresis controller (5 A)

Table 2. Comparison of % THD for various inverter currents

Inverter current (in A)	Adaptive hysteresis band current control	Hysteresis band current control
2	5.67	7.83
3	3.79	4.59
4	3.12	3.65
5	2.94	3.19
6	2.80	3.58
7	2.54	3.35
8	3.08	3.3
9	3.20	3.32
10	2.92	2.42

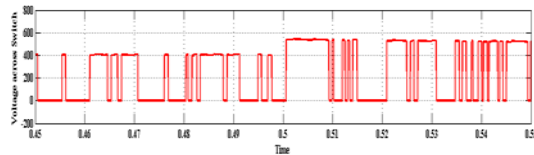


Figure 13. Voltage across a switch with hysteresis controller

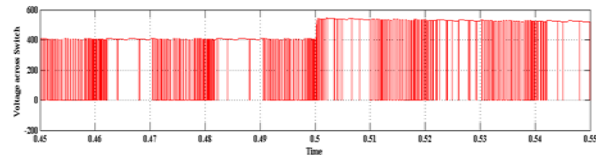


Figure 14. Voltage across switch with a novel hysteresis controller

4. CONCLUSION

In this paper both hysteresis and adaptive hysteresis band current controllers are implemented to the PV inverter tied to grid. In case of the adaptive hysteresis band current controller, the switching frequency is maintained almost constant. The adaptive hysteresis band controller changes the bandwidth based on the modulating frequency, supply voltage, input DC voltage and slope of the reference current, switching frequency is all most all constant. % THD of the grid current is also low with the adaptive hysteresis band controller. This technique can be suggested to control the power in case of micro grid application where current control is required.

REFERENCES

- [1] I. Made Ginarsa, Agung Budi Muljono, I. Made Ari Nnartha, Sultan Sultan, "Transient response improvement of direct current using supplementary control based on ANFIS for rectifier in HVDC," *International Journal of Power Electronics and Drive Systems (IJPEDS)*, vol. 11, no. 4, pp. 2107-2115, 2019.
- [2] Khayat, M. Naderi, Q. Shafiee, Y. Batmani, M. Fathi, J. M. Guerrero, and H. Bevrani, "Decentralized optimal frequency control in autonomous microgrids," *IEEE Transactions on Power Systems*, vol. 34, no. 3, pp. 2345-2353, 2019.
- [3] Bouafia Saber, Benaissa Abdelkader, Bouzidi Mansour, Barkat Said, "Sliding Mode Control of Three Levels Back-To-Back VSC-HVDC System Using Space Vector Modulation," *International Journal of Power Electronics and Drive Systems (IJPEDS)*, vol. 4, no. 2, pp. 256-273, 2014.
- [4] Mohamed S. Ghayad, Niveen M. Badra, Almoataz Y. Abdelaziz, Mahmoud A. Attia, "Reactive power control to enhance the VSC-HVDC system performance under faulty and normal conditions," *International Journal of Applied Power Engineering (IJAPE)*, vol. 8, no. 2, pp. 145-158, 2019.
- [5] P. Kumar Rath and K. Charan Bhuyan, "Vector Control of VSC HVDC System under Single Line to Ground Fault Condition," *International Journal of Applied Power Engineering (IJAPE)*, vol. 7, no. 1, pp. 59-64, 2018.
- [6] S. Bolognani and S. Zampieri, "A Distributed Control Strategy for Reactive Power Compensation in Smart Microgrids," *IEEE Transactions on Automatic Control*, vol. 58, no. 11, pp. 2818-2833, 2013.
- [7] Zhang Zhaoyun, Zhao Wenjun, Yang Mei, Kang Li, Zhang Zhi, Zhao Yang, Liu Guozhong, Yao Na, "Application Of Micro-Grid Control System In Smart Park," *The Journal of Engineering*, vol. 2019, no. 16, pp. 3116-3119, 2019.
- [8] T. Dragicevic, D. Wu, Q. Shafiee, L. Meng, "Distributed and decentralized control architectures for converter-interfaced microgrids," *Chinese Journal of Electrical Engineering*, vol. 3, no. 2, pp. 41-52, 2017.
- [9] Bidram and A. Davoudi, "Hierarchical Structure of Microgrids Control System," *IEEE Transactions on Smart Grid*, vol. 3, no. 4, pp. 1963-1976, 2012.
- [10] L. Meng *et al.*, "Review on Control of DC Microgrids," *IEEE Journal of Emerging and Selected Topics in Power Electronics*, vol. 5, no. 3, pp. 928-948, 2017.
- [11] R. Heyderi, M. Alhasheem, T. Dragicevic, and F. Blaabjerg, "Model predictive control approach for distributed hierarchical control of vsc-based microgrids," *2018 20th European Conference on Power Electronics and Applications (EPE'18 ECCE Europe)*, Riga, 2018, pp. 1-8.
- [12] W. Gu, G. Lou, W. Tan, and X. Yuan, "A nonlinear state estimator-based decentralized secondary voltage control scheme for autonomous microgrids," *IEEE Transactions on Power Systems*, vol. 32, no. 6, pp. 4794-4804, 2017.
- [13] Baoquan Liu, Fang Zhuo, Yixin Zhu, and Hao Yi, "System Operation and Energy Management of A Renewable Energy-Based Dc Micro-Grid for High Penetration Depth Application," *IEEE Transactions on Smart Grid*, vol. 6, no. 3, pp. 1147-1155, 2015.
- [14] Harshitha, H. M., Dawnee, S., and Kumaran, K., "Comparative study of fixed hysteresis band current controller and adaptive hysteresis band current controller for performance analysis of induction motor," *2017 International Conference on Energy, Communication, Data Analytics and Soft Computing (ICECDS)*, Chennai, 2017, pp. 552-558.
- [15] R. S. Ravi Sankar, S. V. Jaya Kumar, K. K. Deepika, "Model Predictive Current Control of Grid Connected PV System," *Indonesian Journal of Electrical Engineering and Computer Science (IJECS)*, vol. 2, no. 2, pp. 285-296, 2016.
- [16] S. Changchien, T. J. Liang, J. F. Chen and L. S. Yang, "Novel High Step-Up DC-DC Converter for Fuel Cell Energy Conversion System," *IEEE Transactions on Industrial Electronics*, vol. 57, no. 6, pp. 2007-2017, 2010.
- [17] R. S. Ravi Sankar, S. V. Jaya Kumar, G. M. Rao, "Adaptive Fuzzy PI Current Control of Grid Interact PV Inverter," *International Journal of Electrical and Computer Engineering (IJECE)*, vol. 8, no. 1, pp. 472-482, 2018.
- [18] E. Román, R. Alonso, P. Ibañez, S. Elorduizapatarietxe, D. Goitia, "Intelligent PV Module for Grid-Connected PV Systems," *IEEE Transactions on Industrial Electronics*, vol. 53, no. 4, pp. 1066-1073, 2006.

- [19] R. S. Ravi Sankar, S. V. Jaya Kumar, K. K. Deepika, "Flexible Power Regulation of Grid-Connected Inverters for PV Systems Using Model Predictive Direct Power Control," *Indonesian Journal of Electrical Engineering and Computer Science (IJECS)*, vol. 4, no. 3, pp. 508-519, 2016.
- [20] A. Rahim and J. Selvaraj, "Multistring Five-Level Inverter with Novel PWM Control Scheme for PV Application," *IEEE Transactions on Industrial Electronics*, vol. 57, no. 6, pp. 2111-2123, 2010.
- [21] H. Akagi and K. Iozaki, "A Hybrid Active Filter for a Three-Phase 12-Pulse Diode Rectifier Used as the Front End of a Medium-Voltage Motor Drive," *IEEE Transactions on Power Electronics*, vol. 27, no. 1, pp. 69-77, 2012.
- [22] N. Flourentzou and Vassilios. G. Agelidis, "Optimized Modulation for AC-DC Harmonic Immunity in VSC HVDC Transmission," *IEEE Transactions on Power Delivery*, vol. 25, no. 3, pp. 1713-1720, 2010.
- [23] Mohamed A. Eltawi, and Zhengming Zhao, "MPPT techniques for photovoltaic applications," *Renewable and Sustainable Energy Reviews*, vol. 25, pp. 793-813, 2013.
- [24] K. K. Deepika, G. K. Rao, J. Vijaya Kumar, R. S. Ravi Sankar, "Enhancement of Voltage Regulation using a 7-Level Inverter based Electric Spring with Reduced Number of Switches," *International Journal of Power Electronics and Drive Systems (IJPEDS)*, vol. 11, no. 2, pp. 555-565, 2020.
- [25] Y. Jiang, A. Abu Qahouq, M. Orabi, "MATLAB/Pspice Hybrid Simulation Modeling of Solar PV Cell/Module," *2011 Twenty-Sixth Annual IEEE Applied Power Electronics Conference and Exposition (APEC)*, Fort Worth, TX, USA, 2011, pp. 1244-1250.
- [26] H. Akagi A. Nabae, S. Atoh, "Control strategy of active power filters using multiple voltage-source PWM converters," *IEEE Transactions on Industry Applications*, vol. IA-22, no. 3, pp. 460-465, 1986.
- [27] Afonso, Couto, J. Martins, "Active Filters with Control Based on the p-q Theory," *IEEE Industrial Electronics Society Newsletter*, vol. 47, no. 3, pp. 5-10, 2000.
- [28] B.K. Bose, "An adaptive hysteresis band current control technique of a voltage feed PWM inverter for machine drive system," *IEEE Transactions on Industrial Electronics*, vol. 37, no. 5, pp. 402-408, 1990.
- [29] We. Dai, Y. Dai, T. Zhong, "A New Method for Harmonic and Reactive Power Compensation," *2008 IEEE International Conference on Industrial Technology, Chengdu, China*, 2008, pp. 1-5.
- [30] Prusty, S. R., Ram, S. K., Subudhi, B. D, Mahapatra, K. K., "Performance analysis of adaptive band hysteresis current controller for shunt active power filter," *2011 International Conference on Emerging Trends in Electrical and Computer Technology*, Nagercoil, India, 2011, pp. 425-429.
- [31] Murat Kale, Engin Ozdemir, "A Novel Adaptive Hysteresis Band Current Controller for Shunt Active Power Filter," *Proceedings of 2003 IEEE Conference on Control Applications, 2003 (CCA 2003)*, vol. 2, Istanbul, Turkey, 2003, pp. 1118-1123.

BIOGRAPHIES OF AUTHORS



R. S. Ravi Sankar Currently working as Associate Professor in the department of EEE in Vignan's Institute of Information Technology, Visakhapatnam, Andhra Pradesh, India. Received his Bachelors, Masters and Doctoral degree from Institution of Engineers, JNTU Hyderabad, JNTU Ananthapuram. His research interests include power quality in distribution systems, Renewable energy Sources , electric drives



Allam Venkatesh was born on June 10th, 1992 in Visakhapatnam, Andhra Pradesh, India. He received Bachelor of Engineering (B.E), in field of Electrical and Electronics Engineering, from Andhra University, Visakhapatnam, India, in 2013. He completed his Masters of Technology (M.Tech.), in field of Power and Industrial Drives, from Vignan's Institute of Information Technology, Affiliated to JNTU Kakinada, Andhra Pradesh in 2017. Currently working as Assistant Professor in Department of Electrical and Electronics in Vignan's Institute of Information Technology, Visakhapatnam. His research interests lie in the area of Current control techniques employed in the area of controlling Grid connected Inverter, Stability Analysis.



K. K. Deepika received her B.Tech. degree in Electrical and Electronics Engineering from Bapatla Engineering College, Guntur. She received her M.Tech. degree in Power Systems and Automation from GITAM University. She is currently pursuing her Ph. D. degree in Electrical Engineering at KLEF, Vijayawada, Andhra Pradesh, India. She is working as Assistant Professor in the Department of EEE in Vignan's Institute of Information Technology, Visakhapatnam, Andhra Pradesh, India. Her research interests include power quality in distribution systems, Renewable energy Sources and Demand Side Management.